Photochemistry and Photobiology, 2004, 80: 78–83

Effects of UV-B Irradiation on a Marine Microecosystem¶

Roberto Marangoni*, Nicola Messina, Domenico Gioffré and Giuliano Colombetti
Istituto di Biofisica del C.N.R., Area della Ricerca di Pisa, Via G. Moruzzi 1, Pisa, Italy

Received 14 August 2003; accepted 10 March 2004

ABSTRACT

Purpose of this work was to study the effect of UV irradiation on a microecosystem consisting of several interacting species. The system chosen was of a hypersaline type, where all the species present live at high salt concentration; it comprises different bacteria; a producer, the photosynthetic green alga *Dunaliella salina*; and a consumer, the ciliated protozoan *Fabrea salina*, which form a complete food chain. We were able to establish the initial conditions that give rise to a self-sustaining microecosystem, stable for at least 3 weeks. We then determined the effect of UV irradiation on this microecosystem under laboratory-controlled conditions, in particular by measuring the critical UV exposure for the two main components of the microecosystem (algae and protozoa) under UV-B irradiances comparable to those of solar irradiation. In our experiments, we varied irradiance, total dose and spectral composition of the actinic light. The critical doses at irradiances of the order of 56 kJ/m^2 (typical average daily irradiance in a sunny summer day in Pisa), measured for each main component of the microecosystem (algae and ciliates), turned out to be around 70 kJ/m^2 for ciliates and 50 kJ/m^2 for *D. salina*. By exposing microecosystems to daily UV-B irradiances of the order of 8 kJ/m^2 (typical average daily irradiance in a sunny winter day in Pisa), we found no effect at total doses of the order of the critical doses at high irradiances, showing that the reciprocity law does not hold. We have also measured a preliminary spectral-sensitive curve of the UV effects, which shows an exponential decay with wavelength.

INTRODUCTION

There is a complex dynamic interaction of solar radiation, atmosphere composition and living organisms. The first oxygen-free atmosphere (under which the early organisms had to possess strong defense strategies against UV irradiation, see Ref. 1) was changed by the emergence of life (2,3) into the present, oxygen-containing atmosphere, impermeable to UV-C and partly also to UV-B. There is now the danger that the atmosphere could become more permeable to UV-B because of the reduction of the ozone layer (the so-called ozone hole problem) caused by anthropic activities (4–5).

UV-B radiation is known to affect living organisms because of its ability to interact with the most important biological macromolecules, such as nucleic acids, proteins and lipids (6–8). In the past 10–15 years, the problem of ozone depletion has followed two main research lines, one devoted to the monitoring of either the stratospheric ozone concentration (*e.g.* NASA/TOMS project [9,10]) or the solar radiation reaching the biosphere (*e.g.* EU ELDONET project [11–13]) and the other oriented toward the assessments of the biological effects of UV-B radiation on cellular and subcellular apparatus. By putting together the information derived from these different approaches, one can possibly draw realistic predictions on how an increased UV-B permeation could alter the global ecosystem and in which direction.

This would require the monitoring of ecosystems and establishing a relationship between their changes and the UV-B doses received, a very complex task to accomplish. Only a few studies have been performed *in situ*, and most of them are focused on only a few species (see, for instance, 14–21).

On the contrary, there is a large number of laboratory studies that are concerned with the effects of UV on selected organisms, from lower (bacteria, algae and protozoa) to higher (plant and animals, including humans) ones. The studies on microorganisms are generally based on a similar experimental approach: a small volume of a single-species culture is exposed to UV irradiation, and some fitness parameters (from cell survival to motility, from photoresponsiveness to photosynthetic efficiency, etc.) are measured before and after UV exposure. A quantitative evaluation of the UV-induced damage can be obtained (for a general review, see Refs. 22–24) by a comparison of the values determined before and after irradiation.

These studies have demonstrated the influence of UV-B radiations on a large variety of biological processes, from thymine dimer formation (25,26) to a reduced photosynthetic efficiency (27–29) to an impairment of motile and photomotile functions (24,30–33). The results of these studies have some drawbacks. First, the critical UV doses for cell survival (or for the damage caused to important cellular functions), deduced from dose–damage curves determined in single-cell studies, are low if compared with the UV doses recorded in a normal sunny day (13,24). This implies that the exposure conditions used in these experiments are far from those of a real ecosystem. Second, it is difficult to predict the behavior of a complex ecosystem starting from studies focused on only a single species.

Studies on single species have, however, demonstrated that the resistance against UV varies widely among different microorganisms. This suggests that UV-resistant species might take advantage

¶Posted on the website on 7 April 2004
*To whom correspondence should be addressed: Istituto di Biofisica del C.N.R., Area della Ricerca di Pisa, Via G. Moruzzi 1, 56124 Pisa, Italy. Fax: 39-050-3152760; e-mail: roberto.marangoni@ibf.cnr.it
Abbreviation: ANOVA, analysis of variance.

of an increased UV-B permeation, whereas nonresistant species could be eliminated. A better approach would require the investigation of real ecosystems, which is very difficult to do because there are many different components and it is very hard to establish quantitative relationships between doses received and relative damage for each species. Some works presented in the literature have explored these problems (34–36).

To try to overcome these difficulties, we have designed a simple, but realistic, laboratory model, where complexity is tractable and both the irradiation conditions and the presence of several interacting species are closer to those of a real ecosystem.

In this article, we present and discuss the effects of UV radiation on self-sustaining marine microecosystems, comprising bacteria, algae and protozoa. These microecosystems have a great stability and can be used as suitable tools to observe phenomena that usually take place in large-scale systems, while their complexity remains tractable. We have measured the effects of UV radiation on single species and on system stability, by exploring different irradiation conditions, and determined preliminary spectral-sensitivity curves.

MATERIALS AND METHODS

The microecosystem

The microecosystem designed belongs to the hypersaline type, where all the species live at high salt concentration (from 0.35% to 0.80% NaCl), thus reducing possible bacterial contamination. It consists of a primary producer, the green flagellated alga *Dunaliella salina*; a primary consumer, the ciliated protozoan *Fabrea salina*; and some bacteria, not identified taxonomically, that are present in the waters of the salt marsh in Torre Colimena (TA, Italy), where the protozoa live freely. Both algae and protozoa were independently cultured in our laboratories; this was not necessary for bacteria because they always accompany the cultures of *F. salina*.

Even if our microecosystem is quite simple, it is relevant for ecological studies because it is formed by protozoa and algae that are the most important dispensers of oxygen, food and energy in the world (37).

Dunaliella salina*: basic aspects and cultures. D. salina* is a biflagellated green alga belonging to the order Volvocales. Under unsuitable environmental conditions, it can enter a defense stage called "palmella," in which several cells are grouped together surrounded by a large amount of secreted gel. In this stage, the cells lose their motile capability but seem to be more resistant to environmental stresses.

D. salina was cultivated in the growth medium suggested by Johnson *et al.* (38) continuously bubbled with air in a light–dark cycle of 15:9 h at a constant temperature of 23°C. The *D. salina* used to feed the protozoa were washed two times by centrifugation; the pellet was then resuspended in the culture medium of the ciliates and added to their culture.

Fabrea salina*: basic aspects and cultures. F. salina* responds to light stimulation, showing both a step-up photophobic response and positive phototaxis (39–41). Its resistance against UV irradiation was found to be significantly greater than that of other ciliates in early studies (42), and, more recently, the action spectrum of the UV-induced damages on motility and photomotility was determined (30). *F. salina* possesses a defense stage called "cyst," which it can enter when the environmental conditions become unsuitable for survival. The morphology of the cysts and the incystment and excystment mechanism have been studied in detail (43). *F. salina* were grown in artificial seawater (the composition of which has been reported in detail by Marangoni *et al.* [40]) in a light–dark cycle of 15:9 h at a constant temperature of 23°C.

Microecosystem seeding and maintenance. The microecosystems used had a volume of 90 mL and was set in small glass vessels. We determined that the optimal ratio between protozoa and algae leading to a stable microecosystem is about 1:10 000 (one protozoan to 10 000 algae). These microecosystems were stable for at least 3 weeks, in some cases up to several months (with a maximum of 8 months).

Identical microecosystems were obtained by mixing algae and protozoa in the required proportion and, thereafter, by randomly dividing this large microecosystem into several small containers. Most of the experiments presented in this article have been performed by seeding five identical microecosystems. Once seeded, the microecosystems were maintained in a dark–light cycle (9:15 h, respectively) in a temperature-constant box (28°C). The samples taken to count cells were added back to the microecosystem as much as possible to keep volume and cell density constant.

Irradiation system and protocols

The vessels containing the microecosystem were placed in irradiation boxes in a temperature-controlled room; an electric fan removed the hot air formed inside the box, keeping the temperature almost constant at 28°C. The excitation light was provided by Philips TL40W/12 UV-B–emitting fluorescent tubes and Philips TLD36W/54 visible light–emitting fluorescent tubes. The vessels containing the microecosystems were surrounded by opaque containers, covered with cutoff filters, which were chosen to vary the spectral composition of the polychromatic light reaching the samples.

To check the validity of the reciprocity law, we varied the irradiation doses supplied to samples by using different numbers of fluorescent tubes or different exposure times. The irradiation experiments were performed in parallel by placing in the irradiation box a certain number of identical microecosystems and covering them with different cutoff filters. Some of the samples were covered by a GG400 cutoff filter that transmits only visible light and were taken as control samples. UV-B radiation was supplied in the middle of the light phase of the light–dark cycle.

Cell counting procedures

Protozoa were counted directly under a microscope by taking each time 1 mL volume from a microecosystem and placing it in a small glass container. When the counting procedure was completed, the sample was added back to the vessel it had been taken from (see above).

Algae were counted both directly, by means of a Thoma chamber under a Leitz Laborlux S microscope, and indirectly, by measuring the light scattered at 520 nm in a spectrophotometer (JASCO UVIDEC 510). A calibration curve was built by comparing cell counts and scattering values for the same algal concentrations, after correcting for bacterial concentration. This is necessary because a part of the light scattered by the sample is due to the presence of bacteria. We separated the bacterial component by filtration on Sartorius 0.45 μm cellulose nitrate filters, which keep protozoa and algae and filter out bacteria.

We then measured the light scattered at 520 nm by the bacterial suspension. This value was subtracted from the value measured on the whole sample (algae and bacteria) at each determination to obtain the corrected calibration curve needed. No calibration curves were determined for bacteria because we were not interested in the absolute number of bacteria present in the microecosystem but only in its relative temporal variations.

UV-irradiation protocols

We performed different series of UV-B exposures of these microecosystems by varying irradiance, total dose and spectral composition of the actinic light. We tested in particular two sets of fluence rates. The first set is of the same order of magnitude of the values recorded for solar irradiance in Pisa on an average day in July 1999; this irradiation condition will be referred to as "high-dose" exposure. The second set is about one-half the solar irradiance in Pisa on an average day in January 1999; this irradiation condition will be referred to as "low-dose" exposure. Both the reference values of solar irradiance are taken from the database of the ELDONET project (13,44). In the following, we give a detailed description of the protocols of sample irradiation.

High-dose UV exposure series. Five identical microecosystems were exposed to strong UV irradiance, on a daily basis, for 8 days. The microecosystems were covered with the following cutoff filters: WG280, WG295, WG305, WG335 and GG400, respectively. The last sample received only photosynthetically active radiation and, as already mentioned, was taken as control sample. Table 1 indicates the daily dose at each 10 nm wavelength interval falling on the sample as a function of the cutoff filter used to cover that microecosystem and the total dose received.

Low-dose UV-exposure series. Five identical microecosystems were seeded, and the same cutoff filters of the previous experiment were used. The irradiations were performed using the daily doses specified in Table 2. The experiment was run for a period of 20 days.

Statistical analysis

Because we carried out multivariate experiments, we tested the significance of the differences in cellular concentration between samples by one-way

Table 1. Daily doses at each 10 nm interval in the UV-B region supplied to the different samples in the high-dose exposure experimental series. The total dose in the UV-B region for an average day in July 1999 in Pisa, Italy, was about 56 kJ/m^2, as recorded by ELDONET dosimeter (see http://www.eldonet.org)

	Daily doses (supplied in 4 h) for each sample (J/m^2)				
λ (nm)	WG280	WG295	WG305	WG335	GG400
280–290	2077.7	1423.8	216.4	16.7	10.6
290–300	6084.1	4820.5	2290.4	21.9	13.3
300–310	10915.7	9633.0	7491.1	26.1	13.6
310–320	10327.9	9648.7	8985.0	162.7	14.5
Total UV-B	29405.4	25526.0	18982.9	227.4	52.0

analysis of variance (ANOVA) tests under the null hypothesis that the concentrations of algae and ciliates are the same between different samples.

RESULTS

In unperturbed conditions, the time variation in the number of cells of the different components of originally identical microecosystems is the same (within experimental errors) for all for a period of at least 3 weeks.

This does not mean that the number of cells remains constant: all the microecosystems show a predator–prey dynamics (45,46), with oscillations of both the number of algae (prey) and ciliates (predator); these oscillations, however, are very similar in all the identically seeded microorganisms, up to 3 weeks from seeding.

UV-exposure effects

High-dose series. The time course of the concentration of the main species (protozoa and algae) of the control sample (covered by GG400) is consistent with the typical predator–prey dynamics of untreated samples. On the contrary, the WG280 sample shows a rapid decrease in the number of both algae and protozoa, which is followed by an unrecoverable decay of the whole microecosystem after the third day of irradiation. Figure 1 shows a comparison between WG280- and GG400-irradiated samples: whereas the latter shows the typical oscillations in the number of producers and consumers (characteristic of the predator–prey dynamics of the microecosystem), the former shows that the number of both components tends toward zero. Figure 1 shows also the time course of bacterial concentration.

We then estimated the UV-induced damage on each component of the microecosystem, based on fact that, in the absence of perturbation, the same number of cells for each component is

Table 2. Daily doses at each 10 nm interval in the UV-B region supplied to the different samples in the low-dose exposure experimental series. In January 1999, the ELDONET instruments recorded in Pisa an average daily dose of 8 kJ/m^2 in the UV-B region

	Daily doses (supplied in 4 h) for each sample (J/m^2)				
λ (nm)	WG280	WG295	WG305	WG335	GG400
280–290	139.5	90.3	8.5	3.0	2.4
290–300	599.2	443.5	130.9	4.3	3.3
300–310	1269.4	1070.5	687.1	5.6	3.3
310–320	1676.4	1528.1	1315.6	111.1	3.5
Total UV-B	3684.5	3132.4	2142.1	124.0	12.5

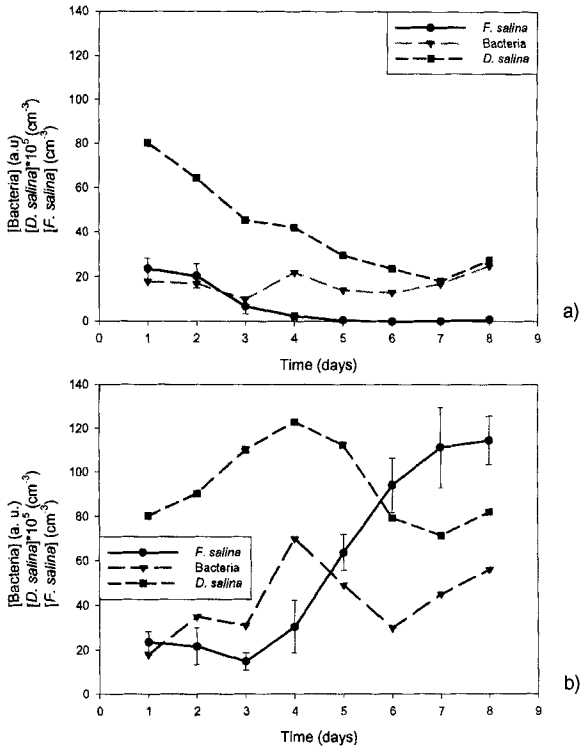

Figure 1. Time course of the concentrations of producers, consumers and bacteria for two microecosystems irradiated under the WG280 (a) and GG400 (b) filters, respectively, in the high-dose experimental series. The ordinate represents the concentration of cells and the abscissa the irradiation time in days.

present in all the originally identical microecosystems, as described above in Materials and Methods. The damage due to irradiation in a microecosystem can thus be estimated by comparing the number of cells of the considered species with that of those exposed only to visible light.

In specific analysis for the consumers (*F. salina*), we calculated, for each day of irradiation, the ratio between the concentration of consumers measured in the various samples and the concentration recorded, for the same day, in the control sample exposed only

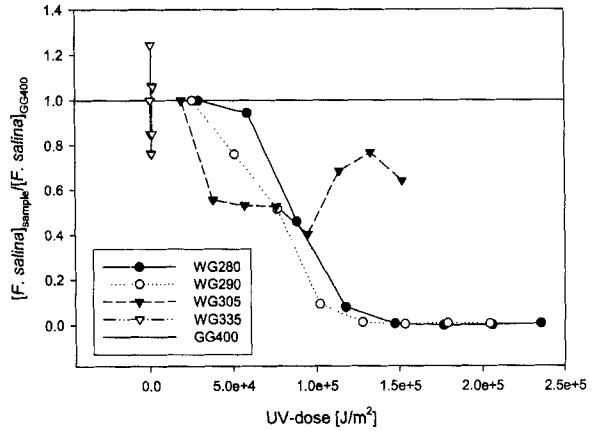

Figure 2. Diagram of the dose–damage relationship for the consumers (*Fabrea salina*) for all the samples used in the high-dose experimental series. The x-axis represents the total UV-B irradiation doses. The y-axis represents the relative cell concentration with respect to that in the sample irradiated under the GG400 filter. Error bars are not visible because of the y-scale chosen.

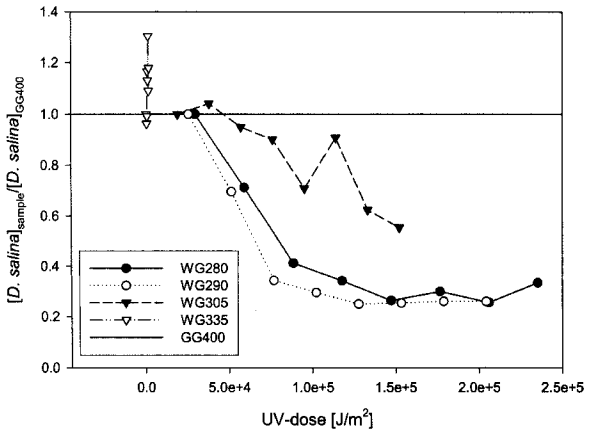

Figure 3. Diagram of the dose–damage relationship for the producers (*Dunaliella salina*) for all the samples used during the high-dose experimental series. Data and axes are arranged as in the previous figure.

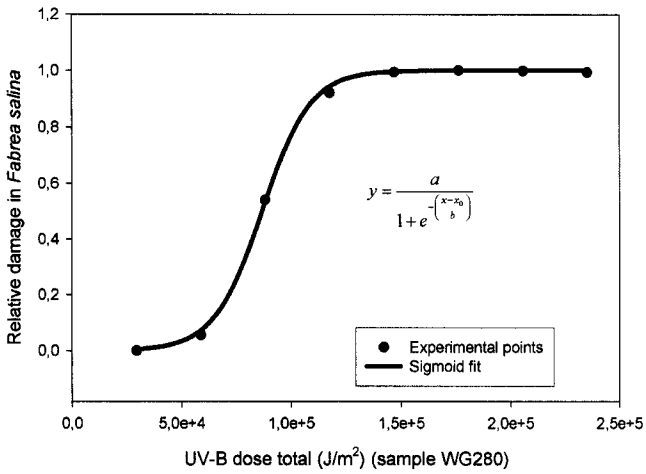

Figure 4. Dose–damage relationship for *Fabrea salina* in the WG280 sample in the high-dose experimental series. The experimental points follow a sigmoid trend, as confirmed by the sigmoid fit, the formula of which is displayed inside the box. Error bars are not visible at this y-axis scale used.

to visible light (GG400). Figure 2 shows the values of this ratio computed for all the samples. Figure 3 shows the same for producers.

It can be seen that WG335 sample always shows a behavior similar to that of GG400, and that the difference from the control samples increases moving toward the WG280 sample, which has received the greatest total amount of UV-B doses.

In the specific analysis for the producers (*D. salina*) similar results were obtained, the main difference being that lower levels of irradiance were enough to severely compromise their survival.

Low-dose series. No UV-induced effects are detectable in the low-dose experiments; all the damage plots show, therefore, a curve almost constant around the value of 1 (data not shown).

UV effects as a function of the starting time of irradiation with respect to the phase of the predator–prey cycle. The rationale of this experiment was to look for a possible correlation between the phase of the predator–prey cycle of the microecosystem and the time at which UV irradiation is started. We seeded five different microecosystems the first day: four of them were exposed to GG400 light and only one to WG280 radiation. Each subsequent day, only one of the remaining GG400 filter was replaced by a WG280 filter, so that the different samples were irradiated with WG280 light at different time points in their life cycle. The fourth day only one sample was exposed to GG400 light. We then measured the time course of the damage caused to different microecosystems and found that the only important factor was the exposure dose, whereas there seemed to be no dependence on the phase of the predator–prey cycle (data not shown).

DISCUSSION

Bacterial concentration time course and contribution

We were unable to find any meaningful correlation between the concentration of bacteria and those of the two other components of the microecosystem. This might seem surprising but can be understood, if we take into account that we are dealing with a composite pool of bacteria. Even if we did not study in detail its taxonomical composition, there must be at least symbionts of *D. salina* and saprophytic bacteria (this is shown by the fact that dead cells of algae and ciliates disappear with time). These two great classes have population dynamics that are very likely opposite; it is reasonable to think that the symbionts grow better when *D. salina* grows, whereas the saprophytic species grow better when there are many dead cells in the microecosystem. If this holds true, it is clear that there is no reason why the total quantity of bacteria should correlate with that of the other components of the microecosystem. At any rate, the evaluation of the damage of the other components of the microecosystem does not depend on the dynamics of the total bacterial concentration, and therefore we will concentrate our discussion on the dynamics of ciliates and algae.

Statistical studies of damage significance

As already stated, the ANOVA was done under the null hypothesis that all the cellular concentrations are identical. In the high-dose series the null hypothesis cannot be rejected for the first 2 days of measurements; it can be rejected (with $P < 0.05$) starting from the third day and can be rejected with extremely high confidence ($P < 0.0001$) for the results of the last day. This holds true for both algae and ciliates. In the low-dose series, the null hypothesis cannot be rejected in any day for either species.

Reciprocity law

In the low-dose series, the total dose supplied to the samples after 20 days of irradiation is comparable to that supplied to samples irradiated for 3 days in the high-dose series. This can be seen from a comparison of the data given in Tables 1 and 2. Although the high-dose samples are significantly affected by irradiation after 3 days (see above), the low-dose samples are not, thus showing that the reciprocity law does not hold.

Microecosystem dynamics and damage estimation

Even if we limit our considerations to the two main components (*D. salina* and *F. salina*) of the microecosystem, its dynamics are hard to describe formally. This is due to several reasons. First, the small number of cells in our microecosystems makes it difficult to use a deterministic model like the Lotka–Volterra one, which is extremely sensitive to small variation in the number of cells (45). Second, both organisms possess defense stages, which exclude

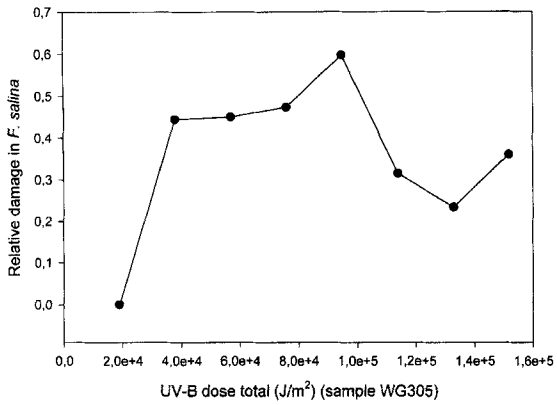

Figure 5. Dose–damage relationship for *Fabrea salina* in the WG305 sample in the high-dose experimental series. The shape of the curve shows three different regions. For values below 10^5 J/m^2, there is an increasing relative damage, as expected. Above this value, the damage apparently decreases, to increase again for irradiation doses greater than 1.4×10^5 J/m^2. This behavior might tentatively be explained in terms of the existence of repair mechanisms. Also in this case, error bars are not visible at this y-axis scale used.

them from the predator–prey competition; any model should, therefore, include also these stages. Finally, there is not enough information for a mathematical model of how the UV-B irradiation changes the main parameters of the populations (fitness, frequencies of entering or exiting the defense stages, etc.).

A possible, better approach could be the application of stochastic predator–prey model (46) because of its robustness with respect to system stability. This will be matter of future work. Here, we limit ourselves to a basic, quantitative analysis of the damage induced by UV-B to each component of the microecosystem, which has allowed us to determine dose–damage relationships. We estimated the relative damage of each component of the microecosystem by means of the following relation:

$$\text{damage}(t_i) = 1 - \frac{[\text{cell}]_{irr}(t_i)}{[\text{cell}]_{vis}(t_i)}$$

where t_i is the time of irradiation, irr, irradiated with UV light and vis, irradiated with visible light.

In other words, the time course of the damage function at day t_i is 1 minus the ratio between the concentrations of the same species in irradiated and control samples. Using this definition, we have investigated the dose–effect curves for UV-induced damages. The relationship for the WG280 sample in the high-dose series is easy to interpret: the experimental data points follow a sigmoid curve, as shown by the high significance of the sigmoid fit to the experimental data (see, in Fig. 4, the dose–effect curve for the ciliate *F. salina*), with an r value of about 0.99 with a $P \ll 0.001$.

Table 3. Values of 1/b coefficient of the sigmoid fit of the dose–damage curves for *Fabrea salina* in each sample of the high-dose series

Sample	1/b value
WG280	9.0×10^{-5}
WG295	6.5×10^{-5}
WG305	2.6×10^{-5}
WG335	5.0×10^{-8}
GG400	0

Evidence for the existence of repair or recovery mechanisms (or both)

The sigmoid fit works well in case of severe damage and, in particular, when the microecosystem is exposed to shorter wavelengths, in particular 280 and 290 nm. On the contrary, for low UV-B doses, or for exposure to wavelengths higher than 290 nm, the dose–damage curves do not show a monotonous, regular shape, increasing in most cases only in their first part (see Fig. 5, the dose–effect curve for *F. salina*). When a certain damage level has been reached, an increase in exposure dose has no further effect on the microecosystem. In other words, the microecosystem remains stable under UV-B exposure, even if in an equilibrium state different from that of a microecosystem exposed to visible light only.

This can be explained by the hypothesis that the cells can activate repair mechanisms with a short delay (of the order of 3 days). These mechanisms arrest the damage, possibly by starting a recovery process of the whole microecosystem, but they seem not to be able to fix the severe damages induced by short-wavelength radiations, as shown by the lack of any recovery in samples irradiated at 280 and 290 nm.

Preliminary evaluation of the spectral sensitivity

The existence of concurrent and opposite phenomena, like damage and repair mechanisms, makes it difficult to build a meaningful action spectrum of the effectiveness of the different wavelengths in damaging the microecosystems. Nevertheless, we made a preliminary evaluation of the effectiveness of the different wavelengths, by applying a sigmoid fit to each dose–damage curve, with the constrain that the fit was limited to the points that give rise to a high acceptability value ($P > 0.95$) for a sigmoid fit. Under this hypothesis, we obtained the data reported in Table 3, which show the value of the term 1/b of the sigmoid fit for each sample in the high-dose experimental series. From this table it can be seen that, as the cutoff filter is shifted toward the visible range, the coefficients show an exponentially decaying trend, in agreement with most of the action spectra for UV-induced damage reported in the literature (22–24,27,30–33).

Acknowledgements—The authors thank Prof. Genuario Belmonte, Dr. Anna Pati and Dr. Salvatore Moscatello of the Department of Biological and Environmental Sciences and Technologies of the University of Lecce, Italy, for their help in collecting *F. salina* cells from the Torre Colimena salt marshes. Thanks are also due to Dr. Francesco Ghetti for his assistance in light measurement.

REFERENCES

1. Kasting, J. F., K. J. Zahnle, J. P. Pinto and A. T. Young (1989) Sulfur, ultraviolet radiation and the early evolution of life. *Origins Life Evol. Biosph.* **19**, 95–108.
2. Canuto, V. M., J. S. Levine, T. R. Augustsson and C. L. Imroff (1982) UV radiation from the young sun and oxygen and ozone levels in prebiological paleoatmosphere. *Nature* **296**, 816–820.
3. Rotschild, L. J. (1999) The influence of UV radiation on protistan evolution. *J. Eukaryot. Microbiol.* **46**, 548–555.
4. World Meteorological Organization (1994) Global Ozone Research and Monitoring Project—Report No. 37. Scientific Assessment of Ozone Depletion: Executive Summary. U.S. Environmental Protection Agency, Washington.
5. Madronich, S., R. L. McKenzie, L. O. Björn and M. M. Caldwell (1998) Changes in biologically active ultraviolet radiation reaching the earth's surface. *J. Photochem. Photobiol. B: Biol.* **46**, 5–19.

6. Dahlback, A., T. Henriksen, S. Larsen and K. Stamnes (1989) Biological UV doses and the effect of an ozone layer depletion. *Photochem. Photobiol.* **49**, 621–625.
7. Biggs, R. H. and M. E. B. Joyner, editors (1994) *Stratospheric Ozone Depletion/UVB Radiation in the Biosphere*. Springer-Verlag, Berlin, Germany.
8. Caldwell, M. M., L. O. Björn, F. J. Bornmann, S. D. Flint, G. Kulandeivelu, A. H. Teramura and M. Tevini (1998) Effects of increased solar ultraviolet radiation on terrestrial ecosystems. *J. Photochem. Photobiol. B: Biol.* **46**, 40–52.
9. Fishman, J. and A. E. Balok (1999) Calculation of daily tropospheric ozone residuals using TOMS and empirically improved SBUV measurements: application to an ozone pollution episode over the eastern United States. *J. Geophys. Res.* **104**, 319–340.
10. Bramstedt, K, J. Gleason, D. Loyola, W. Thomas, A. Bracher, M. Weber and J. P. Burrows (2002) Comparison of total ozone from the satellite instruments GOME and TOMS with measurements from the Dobson network 1996–2000. *Atmos. Chem. Phys. Discuss.* **2**, 1131–1157.
11. Häder, D.-P., M. Lebert, R. Marangoni and G. Colombetti (1999) ELDONET—European light dosimeter network. Hardware and software. *J. Photochem. Photobiol. B: Biol.* **52**, 51–58.
12. Marangoni, R., D. Gioffré, G. Colombetti, M. Lebert and D.-P. Häder (2000) ELDONET—European light dosimeter network. Structure and functions of the ELDONET server. *J. Photochem. Photobiol. B: Biol.* **58**, 178–184.
13. Lebert, M., M. Schuster and D.-P. Häder (2002) The European light dosimeter network: four years of measurements. *J. Photochem. Photobiol. B: Biol.* **66**, 81–87.
14. Kennedy, A. D. (1995) Antarctic terrestrial ecosystem response to global environmental change. *Annu. Rev. Ecol. Syst.* **26**, 683–704.
15. Malloy, K. D., M. A. Holman, D. Mitchell and H. W. Detrich (1997) Solar UVB-induced DNA damage and photoenzymatic DNA repair in Antarctic zooplankton. *Proc. Natl. Acad. Sci. USA* **94**, 1258–1263.
16. Sullivan, J. H. (1997) Effects of increasing UV-B radiation and atmospheric CO_2 on photosynthesis and growth: implications for terrestrial ecosystems. *Plant Ecol.* **128**, 194–206.
17. GwynnJones, D., J. A. Lee and T. V. Callaghan (1997) Effects of enhanced UV-B radiation and elevated carbon dioxide concentrations on a sub-Arctic forest heath ecosystem. *Plant Ecol.* **128**, 242–249.
18. Keller, A. A., P. Hargraves, H. Jeon, G. KleinMacPhee, E. Klos, C. Oviatt and J. Zhang (1997) Effects of ultraviolet-B enhancement on marine trophic levels in a stratified coastal system. *Mar. Biol.* **130**, 277–287.
19. Robakowski, P. and E. Laitat (1999) Effects of an enhanced ultraviolet-B irradiation on photosynthetic apparatus of several forest coniferous tree species from different locations. *Acta Physiol. Plant.* **21**, 283–296.
20. Browman, H. I., C. A. Rodriguez, F. Beland, J. J. Cullen, R. F. Davis, J. H. M. Kouwenberg, P. S. Kuhn, B. McArthur, J. A. Runge, J. F. St-Pierre and R. D. Vetter (2000) Impact of ultraviolet radiation on marine crustacean zooplankton and ichthyoplankton: a synthesis of results from the estuary and Gulf of St. Lawrence, Canada. *Mar. Ecol. Prog. Ser.* **199**, 293–311.
21. Dormann, C. F. and S. J. Woodin (2002) Climate change in the Arctic: using plant functional types in a meta-analysis of field experiments. *Funct. Ecol.* **16**, 4–17.
22. Caldwell, M. M., L. O. Bjorn, J. F. Bornman, S. D. Flint, G. Kulandaivelu, A. H. Teramura and M. Tevini (1998) Effects of increased solar ultraviolet radiation on terrestrial ecosystems. *J. Photochem. Photobiol. B: Biol.* **46**, 40–52.
23. Hader, D. P., H. D. Kumar, R. C. Smith and R. C. Worrest (1998) Effects on aquatic ecosystems. *J. Photochem. Photobiol. B: Biol.* **46**, 53–68.
24. Marangoni, R., F. Marroni, F. Ghetti, D. Gioffre and G. Colombetti (2001) Effects of UV-B in ciliates. In *Environmental UV Radiation: Impact on Ecosystems and Human Health and Predictive Models* (Edited by F. Ghetti), pp. 57–70. NATO-ASI Biosciences series, New York.
25. Douki, T., M. Court and J. Cadet (2000) Electrospray-mass spectrometry characterization and measurement of far-UV-induced thymine photoproducts. *J. Photochem. Photobiol. B: Biol.* **54**, 145–154.
26. Douki, T., M. Court, S. Sauvaigo, F. Odin and J. Cadet (2000) Formation of the main UV-induced thymine dimeric lesions within isolated and cellular DNA as measured by high performance liquid chromatography-tandem mass spectrometry. *J. Biol. Chem.* **275**, 11678–11685.
27. Herrmann, H., D. P. Hader and F. Ghetti (1997) Inhibition of photosynthesis by solar radiation in *Dunaliella salina*: relative efficiencies of UV-B, UV-A and PAR. *Plant Cell Environ.* **20**, 359–365.
28. Neale, P. J., J. J. Cullen and R. F. Davis (1998) Inhibition of marine photosynthesis by ultraviolet radiation: variable sensitivity of phytoplankton in the Weddell-Scotia confluence during the austral spring. *Limnol. Oceanogr.* **43**, 433–448.
29. Krause, G. H., E. Grube, A. Virgo and K. Winter (2003) Sudden exposure to solar UV-B radiation reduces net CO_2 uptake and photosystem I efficiency in shade-acclimated tropical tree seedlings. *Plant Physiol.* **131**, 745–752.
30. Martini, B., R. Marangoni, D. Gioffré and G. Colombetti (1997) Effects of UV-B irradiation on motility and photomotility of the marine ciliate *Fabrea salina*. *J. Photochem. Photobiol. B: Biol.* **39**, 197–203.
31. Sgarbossa, A., S. Lucia, F. Lenci, D. Gioffré, F. Ghetti and G. Checcucci (1995) Effects of UV-B irradiation on motility and photoresponsiveness of the coloured ciliate *Blepharisma japonicum*. *J. Photochem. Photobiol. B: Biol.* **27**, 243–249.
32. Checcucci, G., A. Sgarbossa, D. Gioffrè, F. Lenci and F. Ghetti (1999) Action Spectra for UV-B impacts on *Blepharisma japonicum* motility and photobehavior. *Photochem. Photobiol.* **69**, 86–90.
33. Häder, D. P., S. M. Liu, M. Häder and W. Ullrich (1990) Photoorientation, motility and pigmentation in a freshwater *Peridinium* affected by ultraviolet radiation. *Gen. Physiol. Biophys.* **9**, 361–371.
34. Halac, S., M. Felip, L. Camarero, S. Sommaruga Woghath, R. Psenner, J. Catalan and R. Sommaruga (1997) An *in situ* enclosure experiment to test the solar UVB impact on plankton in a high-altitude mountain lake. I. Lack of effect on phytoplankton species composition and growth. *J. Plankton Res.* **19**, 1671–1686.
35. Sommaruga, R., B. Sattler, A. Oberleiter, A. Wille, S. Sommaruga Wograth, R. Psenner, M. Felip, L. Camarero, S. Pina, R. Girones and J. Catalan (1999) An *in situ* enclosure experiment to test the solar UVB impact on plankton in a high-altitude mountain lake. II. Effects on the microbial food web. *J. Plankton Res.* **21**, 859–876.
36. Sommaruga, R. (2001) The role of solar UV radiation in the ecology of alpine lakes. *J. Photochem. Photobiol. B: Biol.* **62**, 35–42.
37. Finlay, B. J. and T. Fenchel (1996) Ecology: role of ciliates in the natural environment. In *Ciliates: Cells as Organisms* (Edited by J. Hausmann and T. Brandbury), pp. 417–440. G. F. Verlag, New York.
38. Johnson, M. K., E. J. Johnson, R. D. Elroy, H. L. Speer and B. S. Bruff (1968) Effects of salts on the halophilic alga *Dunaliella viridis*. *J. Bacteriol.* **95**, 1461–1468.
39. Marangoni, R., L. Gobbi, F. Verni, G. Albertini and G. Colombetti (1996) Pigment granules and hypericin-like fluorescence in the marine ciliate *Fabrea salina*. *Acta Protozool.* **35**, 177–182.
40. Marangoni, R., S. Puntoni, L. Favati and G. Colombetti (1994) Phototaxis in *Fabrea salina* I. Action spectrum determination. *J. Photochem. Photobiol. B: Biol.* **23**, 149–154.
41. Marangoni, R., R. Cubeddu, P. Taroni, G. Valentini, R. Sorbi, E. Lorenzini and G. Colombetti (1996) Microspectrofluorometry, fluorescence imaging and confocal microscopy of an endogenous pigment of the marine ciliate *Fabrea salina*. *J. Photochem. Photobiol. B: Biol* **34**, 183–189.
42. Moeller, K. M. (1962) On the nature of stentorin. *C. R. Lab. Carlsberg* **32**, 471–498.
43. Repak, A. J. and Q. R. Anderson (1990) The fine structure of encysting salt marsh heterotrich ciliate *Fabrea salina*. *J. Morphol.* **205**, 335–341.
44. On-line database of solar irradiance recorded by ELDONET stations. Available at: http://www.eldonet.org/
45. Huffaker, C. B. (1958) Experimental studies on predation: dispersion factors and predator-prey oscillations. *Hilgardia* **27**, 343–383.
46. Rubinow, S. I. (1974) *Introduction to Mathematical Biology*. John Wiley & Sons, New York.